

# The supernova CSS121015:004244+132827: a clue for understanding super-luminous supernovae.

S. Benetti<sup>1\*</sup>, M. Nicholl<sup>2</sup>, E. Cappellaro<sup>1</sup>, A. Pastorello<sup>1</sup>, S. J. Smartt<sup>2</sup>, N. Elias-Rosa<sup>3</sup>, A. J. Drake<sup>4</sup>, L. Tomasella<sup>1</sup>, M. Turatto<sup>1</sup>, A. Harutyunyan<sup>5</sup>, S. Taubenberger<sup>6</sup>, S. Hachinger<sup>7,1</sup>, A. Morales-Garoffolo<sup>3</sup>, T.-W. Chen<sup>2</sup>, S.G. Djorgovski<sup>4</sup>, M. Fraser<sup>2</sup>, A. Gal-Yam<sup>8</sup>, C. Inserra<sup>2</sup>, P. Mazzali<sup>9,1</sup>, M. L. Pumo<sup>1</sup>, J. Sollerman<sup>10,11</sup>, S. Valenti<sup>12,13</sup>, D. R. Young<sup>2</sup>

<sup>1</sup>INAF - Osservatorio Astronomico di Padova, vicolo dell'Osservatorio 5, I-35122 Padova, Italy

<sup>2</sup>Queen's University Belfast, Belfast BT7 1NN, United Kingdom

<sup>3</sup>Institut de Ciències de l'Espai (IEEC-CSIC), Facultat de Ciències, Campus UAB, 08193 Bellaterra, Spain

<sup>4</sup>California Institute of Technology, 1200 E. California Blvd., CA 91225, USA

<sup>5</sup>Telescopio Nazionale Galileo, Fundación Galileo Galilei - INAF, Rambla José Ana Fernández Pérez, 7, 38712 Breña Baja, TF - Spain

<sup>6</sup>Max-Planck-Institut für Astrophysik, Karl Schwarzschild Str. 1, 85741 Garching bei München, Germany

<sup>7</sup>Institut für Theoretische Physik und Astrophysik, Universität Würzburg, D-97074 Würzburg, Germany

<sup>8</sup>Liverpool John Moores, Liverpool Science Park, IC2 building, 146 Brownlow Hill, Liverpool L3 5RF, UK

<sup>9</sup>Benozio Center for Astrophysics, Weizmann Institute of Science, Rehovot 76100, Israel

<sup>10</sup>Department of Astronomy, AlbaNova Science Center, Stockholm University, SE-106 91 Stockholm, Sweden

<sup>11</sup>The Oskar Klein Centre, AlbaNova, SE-106 91 Stockholm, Sweden

<sup>12</sup>Department of Physics, University of California, Santa Barbara, Broida Hall, Mail Code 9530, Santa Barbara, CA 93106-9530, USA

<sup>13</sup>Las Cumbres Observatory, Global Telescope Network, 6740 Cortona Drive Suite 102, Goleta, CA 93117, USA

Received .....; accepted .....

## ABSTRACT

We present optical photometry and spectra of the super luminous type II Linear-like supernova CSS121015:004244+132827 ( $z=0.2868$ ) spanning epochs from +10 days (rest frame) to more than 200 days after explosion. CSS121015 is one of the brightest supernovae ever observed. Moreover, the collected observations make this one of the most comprehensive data sets for a super luminous supernova (SLSN). The photometric evolution is characterized by a relatively fast rise to maximum ( $\sim 35$  days in the SN rest frame), and by a post-maximum decline which is typical of SNe II-Linear. The light curve shows no sign of a break to an exponential tail.

The early spectral evolution is very fast. The first available spectrum shows a very hot ( $T_{\text{BB}} \sim 17700$  °K) and featureless continuum. The continuum starts to cool down quickly after maximum, and the spectra show the first broad features at  $\sim 57$  days after explosion (rest frame). A broad H $\alpha$  is first detected at  $\sim 80$  days (rest-frame). Narrow, barely-resolved Balmer and [O III] 5007 Å lines, with possibly decreasing strength, are visible along the entire spectral evolution.

The spectra are very similar to other SLSNe with H and also to SN 2005gj, sometimes considered a type Ia interacting with H-rich CSM. The spectra are also similar to those of H deficient SLSNe, after application of a phase stretch based on the relative decline rates of the (pseudo-)bolometric light curves.

The preferred scenario to explain SLSNe (with and without H) is consistent with the interaction of the ejecta with a massive, extended, opaque shell, lost by progenitor decades before the final explosion or major outburst, as an alternative to more exotic explosions (e.g. pair instability supernovae).

**Key words:** Supernovae: general – Supernovae: CSS121015:004244+132827

## 1 INTRODUCTION

Supernovae (SNe), the dramatic and violent end-points of stellar evolution, lie at the heart of some of the most important problems of modern astrophysics. New observational evidence, largely from extensive transient searches (e.g. the Catalina Real-time Transient Survey, the Palomar Transient Factory, PanSTARRS1, La Silla Quest, etc.. Drake et al. 2009; Law et al. 2009; Tonry et al. 2012; Baltay et al. 2013, respectively), is shedding new light both at the bright and faint ends of the SN luminosity distribution. In particular, a number of exceptionally luminous objects (SLSNe) are challenging our existing theoretical picture of the late evolution and explosion of massive stars. It is crucial to understand the nature of these events because, with the next generation of instruments, they may be used to probe star formation and chemical enrichment in the very early Universe (Pop III stars, e.g. Whalen et al. 2013).

While SLSNe are picked out by simple measurement of the total luminosity (Gal-Yam 2012), there is a large diversity in their spectral types and light curve evolution. By volume, they are rare and most have been related to massive stars of some sort. However, whether or not their rarity points to an origin at the top end of the mass function, or to some other characteristics of the progenitor (e.g. extremely low metallicity), is not known. Some SLSNe show clear spectral signatures of hydrogen – usually relatively narrow emission lines, leading to the classification as type II events (e.g. Drake et al. 2011). In only one case (SN 2008es) H shows very broad emission features (Gezari et al. 2009; Miller et al. 2009). Finally, there appears to be a class of SLSNe that do not show H, and spectroscopically evolve to resemble stripped-envelope type Ic SNe (e.g. Quimby et al. 2011; Pastorello et al. 2010b). These have been termed SLSNe-I by Gal-Yam (2012) and super-luminous type Ic SNe by Inserra et al. (2013a). Originally classified as SLSNe by the first secure redshift determinations, they were shown to evolve spectroscopically into type Ic-like SNe on very long timescales by Pastorello et al. (2010b). They were discovered up to redshifts  $\sim 1$  in the deep Pan-STARRS1 Medium Deep Survey (Chomiuk et al. 2011) and a significant effort has been invested to characterize them retrospectively in ongoing surveys (Barbary et al. 2009; Leloudas et al. 2012; Chornock et al. 2013; Lunnan et al. 2013). Cooke et al. (2012) and Howell et al. (2013) extended the discovery of SLSNe up to redshift  $> 1.5$ .

It has been claimed that some of these SLSNe are powered by the radioactive decay of large amounts of  $^{56}\text{Ni}$ , and are therefore the observational counterparts of the long sought pair-instability SNe. These have even been proposed as a class named “SLSN-R” (Gal-Yam 2012). The first example is the bright and slow declining SN 2007bi (Gal-Yam et al. 2009), although Young et al. (2010) suggested that a standard iron-core-collapse origin could not be ruled out (see also Moriya et al. 2013a). Pair-instability SNe are predicted by stellar evolution theory to terminate the lives of stars with mass  $> 140 M_{\odot}$  which have low enough mass-loss rates to retain a large CO-core. However, their existence in the local Universe is not settled, since the observed properties of SLSNe can be explained by different physical processes, including energy input from a newly formed magnetar (Woosley 2010; Dessart et al. 2012; Inserra et al. 2013a;

Nicholl et al. 2013); the accretion onto a proto-neutron star or a black hole (Dexter & Kasen 2013); or interaction of the ejecta with circumstellar material (Blinnikov & Sorokina 2010; Chevalier & Irwin 2011; Ginzburg & Balberg 2012; Moriya et al. 2013a,b,c).

The interaction of the ejecta with CSM is seemingly a frequent phenomenon in massive star explosions, with a number of luminous transients already related to the violent shocks formed when multiple shells collide. This is the case for other kinds of outbursts that can compete with SNe in luminosities and expansion velocities (SN impostors, Van Dyk et al. 2000; Maund et al. 2006; Smith et al. 2011) even if the star survives the event. Eruptive mass loss can build up a dense circumstellar medium (CSM) around a massive star. When the star eventually explodes, the high-velocity ejecta impacts the dense CSM, converting part of its kinetic energy into radiation. The transient becomes very bright, with a luminosity evolution modulated by the density profile of the CSM. When this mechanism is at work it can easily outshine all other radiation sources – making it difficult, if not impossible, to identify the explosion mechanism or even to assess whether an underlying SN has occurred, as in the spectacular case of SN 2009ip (Pastorello et al. 2013; Fraser et al. 2013; Mauerhan et al. 2013; Margutti et al. 2013, and references therein).

This potential for extreme brightness makes ejecta-CSM interaction an appealing physical scenario to explain supernovae with unusually high luminosities (Chevalier & Irwin 2011; Ginzburg & Balberg 2012). This interpretation has been adopted for H-rich SLSNe, such as SN 2008es (Gezari et al. 2009; Miller et al. 2009), and may also be relevant to H-deprived transients (see e.g. Chatzopoulos et al. 2013, and references therein). In fact very recently Ben-Ami et al. (2013) presented a case of a Type Ic supernova whose ejecta started to interact with a massive, hydrogen-free ( $\sim 3M_{\odot}$ ) CSM.

In this paper we report on observations of a new event that appears to support the ejecta-CSM interpretation. CSS121015:004244+132827 (CSS121015 from here on) was first detected by CRTS on Sep. 15, 2012, at a V magnitude of  $\sim 20.0$ , as announced by Drake et al. (2012). They also reported that a spectrum taken with Palomar 5m Telescope + DBSP on Oct 15th UT showed a very blue continuum with no clear emission features, resembling the early spectra of other luminous type-I supernovae detected by CRTS. A follow-up spectroscopic observation by Tomasella et al. (2012), obtained with the Asiago 1.82-m Copernico Telescope + AFOSC, confirmed the very blue, featureless continuum, but also allowed the detection of faint, narrow Balmer emissions from the host galaxy. A redshift of  $\sim 0.286$  was hence derived, making CSS121015 extremely bright ( $\sim -22.5$ ). The spectral appearance was that of a stripped envelope SN such as those discussed in Quimby et al. (2011) and Pastorello et al. (2010b). After this classification, we began an extensive follow-up campaign for CSS121015 in the optical domain, within the frameworks of the Asiago-TNG Supernova follow-up campaign<sup>1</sup> and the Public ESO Spectroscopic Survey of Transient Objects (PESSTO)<sup>2</sup>. In this

<sup>1</sup> <http://sngroup.oapd.inaf.it>

<sup>2</sup> <http://www.pessto.org/pessto/index.py>

paper we present the results of this monitoring campaign and discuss the implications for the SLSNe scenarios.

## 2 REDDENING AND DISTANCE OF CSS121015 AND ITS HOST GALAXY

The host of CSS121015 is a faint galaxy, barely visible in Sloan images (SDSS DR9<sup>3</sup>) (Eisenstein et al. 2011). Using our deeper  $r$ -band frame (see Table 3), we measured an apparent magnitude of  $r \sim 23.0$  for the parent galaxy.

The Galactic reddening towards CSS121015,  $A_B=0.314$ , was taken from the recalibrated infrared-based dust map of Schlafly & Finkbeiner (2011). We assume that the extinction in the host galaxy is negligible, as we detect no sign of narrow interstellar NaID absorption (Turatto, Benetti, & Cappellaro 2003; Poznanski et al. 2012), even in spectra of higher S/N ratio (cf. Section 4).

From the narrow emission lines visible in the spectra with better S/N ratio ( $H\alpha$ ,  $H\beta$  and  $[O III] 5007\text{\AA}$  lines; see Section 4), we derive a mean redshift  $z = 0.2868 \pm 0.0006$ , where the error is the standard deviation of several measurements. Assuming a Planck Universe ( $H_0 = 67.3 \text{ km s}^{-1} \text{ Mpc}^{-1}$ ,  $\Omega_\lambda = 0.685$  and  $\Omega_m = 0.315$  from Ade et al. 2013), the luminosity distance for CSS121015 is  $d_l = 1520 \text{ Mpc}$  and the distance modulus is  $\mu = 40.91 \text{ mag}$ ; these values are used throughout the paper.

Adopting the reddening and the distance modulus discussed above, we infer a magnitude of  $M_r \gtrsim -17.9$  for the faint host galaxy of CSS121015. This supports the claim of Neill et al. (2011) that SLSNe favor low luminosity host galaxies falling on the blue edge of the blue cloud in the color-magnitude diagram (see their Fig. 2), and have moderately low star formation rates and low stellar masses, resulting in high specific star formation rates. This together with the link between galaxy mass and metallicity (Tremonti et al. 2004) suggests that wind-driven mass loss is the factor preventing SLSN explosions in higher-mass, higher-metallicity hosts.

## 3 OPTICAL PHOTOMETRY

Optical imaging data of CSS121015 were obtained using a number of different instrumental configurations. Basic information on these observations is reported in Tables 2 and 3.

The CCD frames were first bias and flat-field corrected in the usual manner. Since some of the data were obtained under non-photometric conditions, we measured relative photometry with respect to local field stars (see Fig. 1), whose magnitudes were computed by averaging estimates obtained on photometric nights.

Ideally, one would like to remove the galaxy background by subtraction of a galaxy “template” (i.e. an image where the SN is absent). In the case of CSS121015, suitable template images were not available for the Johnson-Cousins frames. However, as the host galaxy is quite faint (see Sect. 2), the SN magnitudes could be measured via

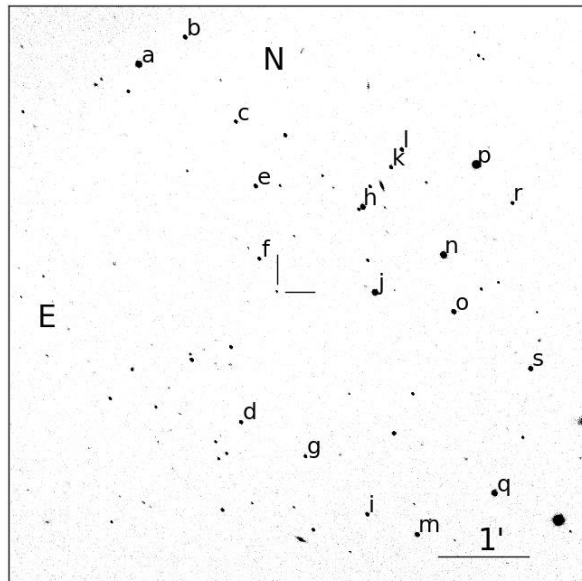


**Figure 1.** CSS121015 supernova and reference stars. This is a TNG+LRS R frame taken on December 25th, 2012. The measured seeing was  $1.5''$ .

PSF-fitting using dedicated, custom-built pipelines (developed by two of us, E.C. and S.V.), consisting of a collection of PYTHON scripts calling standard IRAF tasks (through PYRAF), and specific data analysis tools, such as SEXTRACTOR (for source extraction and classification) and DAOPHOT (for PSF-fitting). In our implementation of the PSF-fitting procedure, an initial estimate of the sky background at the SN location is obtained using a low order polynomial fit to the surrounding region. This is subtracted from the image, before fitting the SN with a PSF model derived from isolated field stars. The fitted source is removed from the original image, an improved estimate of the local background is derived, and the PSF-fitting procedure is iterated. The residuals are visually inspected to validate the fit.

Error estimates were obtained through artificial star experiments, in which a fake star, of similar magnitude to the SN, is placed in the PSF-subtracted residual image in a position close to, but not coincident with, that of the real source. The simulated image is processed through the PSF-fitting procedure. This process is repeated at a number of positions; the dispersion of the magnitude returned by the pipeline is taken as an estimate of the instrumental magnitude error, accounting mainly for the background fitting uncertainty. This is combined (in quadrature) with the PSF-fit error returned by DAOPHOT, and the propagated errors from the photometric calibration.

### 3.1 Johnson-Cousins UBVR photometry

Six photometric nights were used to calibrate the local stellar sequence, introduced in Section 3, against Landolt standard stars (Landolt 1992). The Johnson-Cousins magnitudes of the local standards, and their estimated errors, are shown in Table 1. In addition to standard UBVR filters, CSS121015 was also observed with SDSS filters (cfr.

<sup>3</sup> <http://skyserver.sdss3.org/dr9/en/tools/chart/>

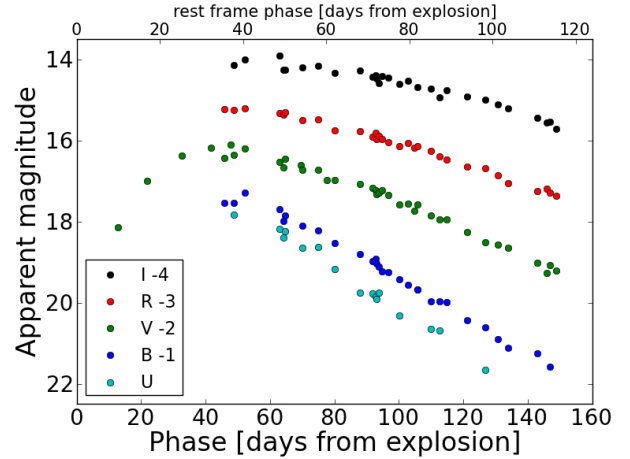
**Table 1.** Magnitudes of local sequence stars identified in Figure 1.

star	RA	Decl	U	errU	B	errB	V	errV	R	errR	I	errI
a	0:42:52.689	13:31:46.32	15.72	0.04	15.73	0.01	15.03	0.01	14.65	0.01	14.25	0.01
b	0:42:49.903	13:32:10.22	17.87	0.02	18.06	0.02	17.32	0.01	16.95	0.01	16.52	0.04
c	0:42:46.848	13:30:55.87			19.09	0.02	18.11	0.01	17.56	0.01	17.01	0.04
d	0:42:46.531	13:26:31.35			19.28	0.01	17.95	0.01	17.18	0.01	16.50	0.01
e	0:42:45.662	13:29:59.14			19.80	0.01	18.12	0.01	17.12	0.01	16.01	0.02
f	0:42:45.450	13:28:55.00			20.44	0.05	18.87	0.01	17.87	0.01	16.64	0.01
g	0:42:42.641	13:26:01.14	19.10	0.08	19.30	0.02	18.53	0.01	18.14	0.01	17.70	0.02
h	0:42:39.203	13:29:40.90			17.01	0.01	16.15	0.01				
i	0:42:38.896	13:25:09.59	17.93	0.01	18.67	0.02	17.84	0.01	17.40	0.01	16.95	0.03
j	0:42:38.450	13:28:25.51	16.27	0.02	16.11	0.01	15.31	0.01	14.89	0.01	14.50	0.02
k	0:42:37.487	13:30:15.87	18.80	0.05	18.78	0.01	17.90	0.01	17.46	0.01	16.94	0.02
l	0:42:36.836	13:30:31.45			18.53	0.02	17.53	0.01	17.01	0.01	16.48	0.03
m	0:42:35.875	13:24:51.53	17.16	0.04	17.45	0.02	16.82	0.01	16.43	0.01	15.95	0.02
n	0:42:34.314	13:28:58.59	16.90	0.01	16.09	0.01	15.05	0.01	14.48	0.01	13.98	0.01
o	0:42:33.686	13:28:08.43	17.47	0.01	17.39	0.01	16.62	0.01	16.21	0.01	15.74	0.02
p	0:42:32.321	13:30:18.29	15.56	0.01	15.10	0.01	14.14	0.01	13.65	0.01		
q	0:42:31.195	13:25:28.07	17.14	0.05	16.66	0.01	15.70	0.01	15.20	0.01		
r	0:42:30.116	13:29:44.29			19.53	0.02	18.48	0.01	17.89	0.01	17.26	0.02
s	0:42:29.068	13:27:18.36	17.71	0.03	17.69	0.01	16.80	0.01			15.78	0.01

Sect. 3.2). In particular, we used the Liverpool Telescope (+ RATCam) to get SDSS-*u*, Johnson-BV and SDSS-*ri*. These instrumental magnitudes were then transformed to Johnson-UBV and Cousins-RI magnitudes using colour equations, again derived through observations of Landolt fields, to enrich the UBVRI light curves. The final SN magnitudes (calibrated in the Vega system) are presented in Table 2. Sometimes the errors are relatively high, mostly because of poor sky transparency and/or poor seeing. The UBVRI light curves are plotted in Figure 2.

Only the V light curve has pre-maximum points. They are from unfiltered (pseudo-V) CRTS magnitudes converted to V following the recipe of Drake et al. (2013). The rising phase is steeper than the post-maximum decline. By fitting a low order polynomial to the observed V-band light curve, we estimate that the maximum occurred on JD =  $2456219 \pm 2$ , at  $V = 18.22 \pm 0.10$  mag. Given the smooth rise shown by the V light curve, we assume that the explosion happened about 10 days (rest frame) before the first detection date (see Table 2), i.e. JD =  $2456174 \pm 10$  (in the observed frame), and this will be used as reference epoch. The big uncertainty in this epoch includes the possibility of an early “plateau”-like break, as seen in the rising light curve of one SLSN (see Leloudas et al. 2012). We prefer to use the explosion, instead of maximum light epoch as reference epoch because this gives more physically meaningful comparisons with other events.

The post-maximum declines are progressively slower as we move from the U to the I band. Starting from maximum light, the observed linear decline rates are  $5.40 \pm 0.20$ ,  $4.53 \pm 0.10$ ,  $3.23 \pm 0.08$ ,  $2.43 \pm 0.08$ , and  $1.92 \pm 0.11$  mag  $(100d)^{-1}$  in U,B,V,R and I, respectively. The declines in all bands are steeper than that of  $^{56}\text{Co}$  decay up to about 110 days after maximum (about 85 days in the SN rest frame), and the light curves never show a break in their decline.

**Figure 2.** Johnson-Cousins U (top), B, V, R and I (bottom) light curves of CSS121015. The phase given is in the observer frame (bottom x-axis) and SN rest-frame (top x-axis).

### 3.2 SDSS *griz* photometry

CSS121015 was observed in the SDSS *griz* bands with the Faulkes North Telescope, equipped with the MEROPE1 and Spectral2 cameras. Table 3 integrates this data with the *ri* data from LT+RATCam, mentioned above, collecting all SDSS photometry. This was reduced with the same recipes used for the Johnson-Cousins photometry. The photometric calibration was achieved by comparing the magnitudes obtained for the stars in the field of CSS121015 with their SDSS magnitudes, and is therefore close to the AB system ( $g, r, i_{\text{SDSS}} \sim g, r, i_{\text{AB}}$ , while  $z_{\text{SDSS}} \sim z_{\text{AB}} - 0.02$  mag<sup>4</sup>).

In the table we also report deep *r* and *i* limits obtained with WHT+ACAM and TNG+LRS more than 200 days (rest frame) after explosion. These will turn out to be very

<sup>4</sup> <http://www.sdss3.org/dr9/algorithms/fluxcal.php#SDSStoAB>

**Table 2.** Johnson-Cousins photometric measurements for CSS121015, calibrated in the Vega system.

date	JD (−2400000)	phase* (days)	U	errU	B	errB	V	errV	R	errR	I	errI	instrument
20120916	56186.74	13(10)					20.14	0.28					CRTS
20120925	56195.87	22(17)					18.99	0.13					CRTS
20121006	56206.72	33(25)					18.37	0.23					CRTS
20121015	56215.74	42(32)					18.18	0.08					CRTS
20121019	56219.92	46(36)			18.53	0.03	18.42	0.02	18.22	0.02			AF
20121021	56221.92	48(37)					18.10	0.05					CRTS
20121022	56222.83	49(38)	17.83	0.04	18.54	0.02	18.35	0.03	18.24	0.02	18.13	0.02	AF
20121026	56226.11	52(40)			18.29	0.20	18.19	0.10	18.20	0.06	18.00	0.07	RAT
20121105	56236.99	63(49)	18.17	0.04	18.70	0.02	18.52	0.02	18.33	0.02	17.91	0.02	AF
20121106	56238.10	64(50)	18.39	0.08	18.99	0.02	18.67	0.02	18.37	0.18	18.26	0.04	EF2
20121107	56238.80	65(50)	18.23	0.03	18.85	0.02	18.45	0.02	18.30	0.02	18.25	0.02	AF
20121112	56243.64	70(54)					18.61	0.05					CRTS
20121112	56244.10	70(54)	18.64	0.09	19.10	0.07	18.73	0.05	18.49	0.12	18.19	0.07	EF2
20121118	56249.05	75(58)	18.62	0.02	19.22	0.02	18.72	0.02	18.47	0.02	18.15	0.02	LRS
20121120	56251.59	78(60)					18.98	0.14					CRTS
20121123	56254.13	80(62)	19.17	0.09	19.52	0.04	18.98	0.02	18.75	0.02	18.34	0.03	EF2
20121130	56261.84 <sup>‡</sup>	88(68)	19.76	0.17	19.81	0.06	19.07	0.02	18.76	0.02	18.27	0.02	RAT
20121204	56265.84	92(71)	19.77	0.17	19.98	0.06	19.16	0.06	18.90	0.04	18.43	0.02	RAT
20121205	56266.85	93(72)	19.85	0.16	19.92	0.04	19.22	0.03	18.81	0.02	18.39	0.02	RAT
20121205	56267.00	93(72)	19.90	0.09	20.03	0.04	19.32	0.05	18.96	0.04	18.46	0.04	EF2
20121206	56267.76	94(73)	19.75	0.22	20.11	0.13	19.28	0.06	18.89	0.03	18.58	0.05	AF
20121207	56268.85	95(74)			20.23	0.04	19.23	0.04	18.96	0.03	18.40	0.03	RAT
20121209	56270.85	97(75)			20.24	0.06	19.34	0.03	19.05	0.02	18.44	0.02	RAT
20121212	56274.10	100(78)	20.31	0.10	20.43	0.04	19.57	0.02	19.13	0.15	18.61	0.05	EF2
20121215	56276.84	103(80)			20.55	0.11	19.56	0.04	19.06	0.03	18.53	0.03	RAT
20121217	56278.81	105(81)					19.74	0.04	19.17	0.04			AF
20121218	56279.87	106(82)			20.67	0.10	19.58	0.03	19.14	0.02	18.68	0.02	RAT
20121218	56279.88	106(82)			20.68	0.13							AF
20121222	56284.00	110(85)	20.64	0.10	20.96	0.11	19.85	0.03	19.26	0.03	18.72	0.02	LRS
20121225	56286.75	113(88)	20.68	0.09	20.97	0.05	19.94	0.03	19.40	0.02	18.93	0.02	LRS
20121227	56288.85	115(89)			20.99	0.14	19.95	0.11	19.47	0.05	18.76	0.02	RAT
20130102	56295.10	121(94)			21.43	0.04	20.26	0.03	19.64	0.03	18.91	0.05	EF2
20130108	56300.75	127(99)	21.65	0.06	21.60	0.02	20.50	0.02	19.69	0.02	19.00	0.02	LRS
20130112	56304.83	131(102)			21.90	0.06	20.56	0.05	19.86	0.03	19.10	0.06	RAT
20130115	56307.88	134(104)			22.12	0.10	20.65	0.18	20.05	0.07	19.20	0.03	RAT
20130124	56316.87	143(111)			22.24	0.26	21.02	0.15	20.25	0.06	19.43	0.02	RAT
20130127	56320.00	146(113)					21.27	0.11	20.18	0.07	19.56	0.17	LRS
20130128	56320.84	147(114)			22.58	0.18	21.08	0.13	20.29	0.06	19.54	0.04	RAT
20130130	56322.74	149(116)					21.21	0.14	20.37	0.06	19.71	0.08	AF

\* - Relative to the estimated epoch of the explosion (JD = 2456174); the phase in parenthesis is in the SN rest frame. The rise to maximum V lasted  $\sim 49$  days ( $\sim 38$  days in the rest frame).

CRTS = Catalina Real-time Transient Survey

AF = Asiago 1.82m Telescope + AFOSC

RAT = Liverpool Telescope + RATCam (SDSS u, r, i and Johnson B, V)

EF2 = ESO-NTT + EFOSC2

LRS = TNG + LRS

‡ for JD=2456264.72 we have also NIR LBT-Lucifer observations (on 2MASS scale): J=18.46  $\pm$  0.05; H=18.34  $\pm$  0.04; K=17.94  $\pm$  0.06.

important in deriving an upper limit to the  $^{56}\text{Ni}$  mass synthesized in the explosion (see Sect. 5). These limits have been obtained with template subtraction. This technique requires that exposures of the field, obtained before the explosion or long after the SN has faded, are available. The templates have to be taken with the same filters used for SN imaging, with high S/N ratio and good seeing. While in principle they should be obtained with the same telescopes as those used for the specific SN observations (to guarantee the same bandpass), in practice archival images with the proper filters in the on-line archives are very welcome. In our case

we were able to retrieve deep pre-discovery exposures in the  $r, i$  bands from SDSS3-DR9.

In template subtraction, the template image is first geometrically registered to the same pixel grid as the SN frame. The PSF of the two images is then matched by means of a convolution kernel determined by comparing a number of reference sources in the field (for this we used HOTPANTS<sup>5</sup>). After matching the photometric scale, the template image is subtracted from the SN image, and a difference image is

<sup>5</sup> <http://www.astro.washington.edu/users/becker/hotpants.html>

obtained. In our case no residuals were detectable in the  $r$ - and  $i$ -band frames at the SN location, so we can only estimate an upper limit to the SN magnitude.

The limits were estimated through artificial star experiments, in which a fake star of a given magnitude is placed in the original frame at the precise position of the source. The process is iterated several times by injecting fainter and fainter fake stars. The limit is given by the magnitude of the fake star that leaves detectable residuals after template subtraction.

#### 4 SPECTROSCOPY

Our spectroscopic observations cover a time interval from day +46 to day +137 (in the observer frame) from the estimated explosion epoch. Table 4 lists the date (column 1), the JD (col. 2), the observed (and rest-frame) phases relative to the explosion (col. 3), the wavelength range (col. 4), instrument used (col. 5), and the resolution as measured from the FWHM of the night-sky lines (col. 6). For some epochs, we co-add near-contemporaneous spectra to improve the S/N.

The spectra were reduced using standard IRAF routines. Extractions were variance-weighted, based on the data values and a poisson/ccd model using the gain and readout-noise parameters. The background at either side of the SN signal was fitted with a low order polynomial and then subtracted. Fluxing and telluric absorption modeling were achieved using observations of spectrophotometric standard stars. For EFOSC spectra, all the previous steps were optimized in a custom-built PYTHON/PYRAF package (PESSTO-NTT pipeline) developed by one of us (S.V.) including also an automatic check of the wavelength calibration using the sky lines. Most spectra have been taken with the slit aligned along the parallactic angle. The flux calibration of the spectra was checked against the photometry (using the IRAF task STSDAS.HST.CALIB.SYNPHOT.CALPHOT) and, when discrepancies occurred, the spectral fluxes were scaled to match the photometry. On nights with fair to good sky conditions, the agreement with photometry was within 15%. A selection of the CSS121015 spectra is shown in Figure 3.

##### 4.1 Spectroscopic evolution and comparison with other SLSNe-II

The early spectra show a very blue continuum ( $T_{\text{BB}} \sim 17700$  K, after reddening and redshift corrections). This becomes progressively redder with phase, reaching a temperature of about 5500 K at 137 days. Initially, the spectra are almost featureless, with the first broad features – mostly due to Fe II lines – becoming visible in the spectrum at +73 days. The spectrum at +49/50 days (see Fig. 3) shows a narrow, barely resolved  $H\alpha$  emission, and no clear broad Balmer features.

However, the high-S/N ratio spectra at phases +101/102 days show a dim and broad (FWMH  $\sim 10000$  km s $^{-1}$ )  $H\alpha$  emission, with the faint, narrow component superimposed (and only marginally resolved) on top. In the blue part of the spectrum, narrow Balmer and [O III] emission lines are also visible. Whether the narrow lines are intrinsic to the SN or are of interstellar origin is difficult to establish, mostly because of the relatively low S/N ratio of

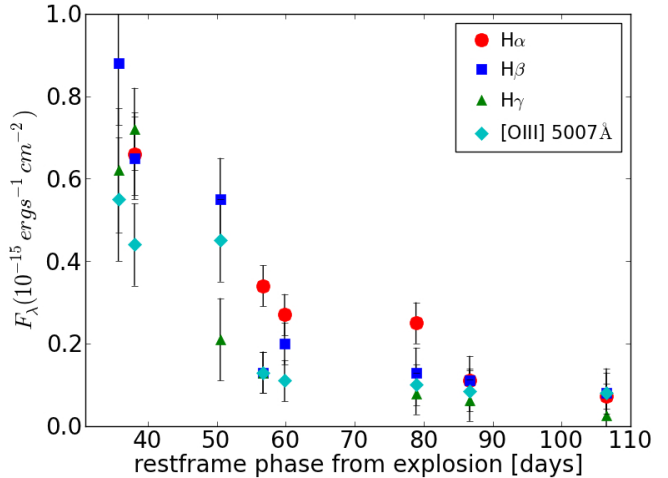


**Figure 4.** Flux evolution of the narrow Balmer and [O III] 5007Å lines.

the first spectra. However, the luminosities of the narrow hydrogen ( $H\alpha$ ,  $H\beta$ , and  $H\gamma$ ) and O III 5007Å line seem to show a smooth decrease (see Figure 4), suggesting that the SN is contributing at least partly to the narrow H and [O III] 5007Å lines. Interestingly, flux variation of [O III] lines has previously been detected in SN IIn (e.g. in Turatto et al. 1993). Given the clear presence of a broad  $H\alpha$  line in the +101/102 days spectra, we may finally classify CSS121015 as a Type II supernova.

At this time, the blue part of the spectrum is dominated by broad metal features, mostly belonging to the Fe group, with some contribution from Ca II H&K and Mg II. The spectra show little evolution between 100 days and the end of our observations, and never show any hint of O, though we detect what may be a weak [Ca II] 7300 Å line. As shown in the upper right panel of Fig. 3, the  $H\alpha$  emission shows a slightly asymmetric, triangular profile, with a red wing extending up to  $v_{ZI} \sim 10000$  km s $^{-1}$ .

In Fig. 5, the CSS121015 spectra are compared with other very bright SNe at similar phases. The comparison SN sample (SNe 2005gj, 2008es, and 2008fz) has been selected using the GELATO comparison tool<sup>6</sup> (Harutyunyan et al. 2008) as the objects that give the best overall match to CSS121015 along its evolution. Up to day  $\sim +40$  (rest frame), the spectra are dominated by a blue continuum, and only the +22 day SN 2005gj spectrum shows some broad-dim features. The broad bump at  $\sim 4600$  Å, visible in the +59/61 days CSS121015 spectrum, is also detected in SN 2008es at a similar phase, while the SN 2008fz spectrum at a slightly later phase (+68 days) shows stronger features. At +78/80 days, the spectra of the four SNe are extraordinarily similar, with the exception of the multi-component  $H\alpha$  profile in SN 2005gj. This SN shows prominent intermediate and narrow line profiles, which suggest the presence of a more extended and diluted CSM. The broad components are similar both in the profile and extension, with terminal velocities of  $\sim 10000$  km s $^{-1}$ . The spectra at late phases also show good agreement, and are all dominated in the blue by

<sup>6</sup> <https://gelato.tng.iac.es>

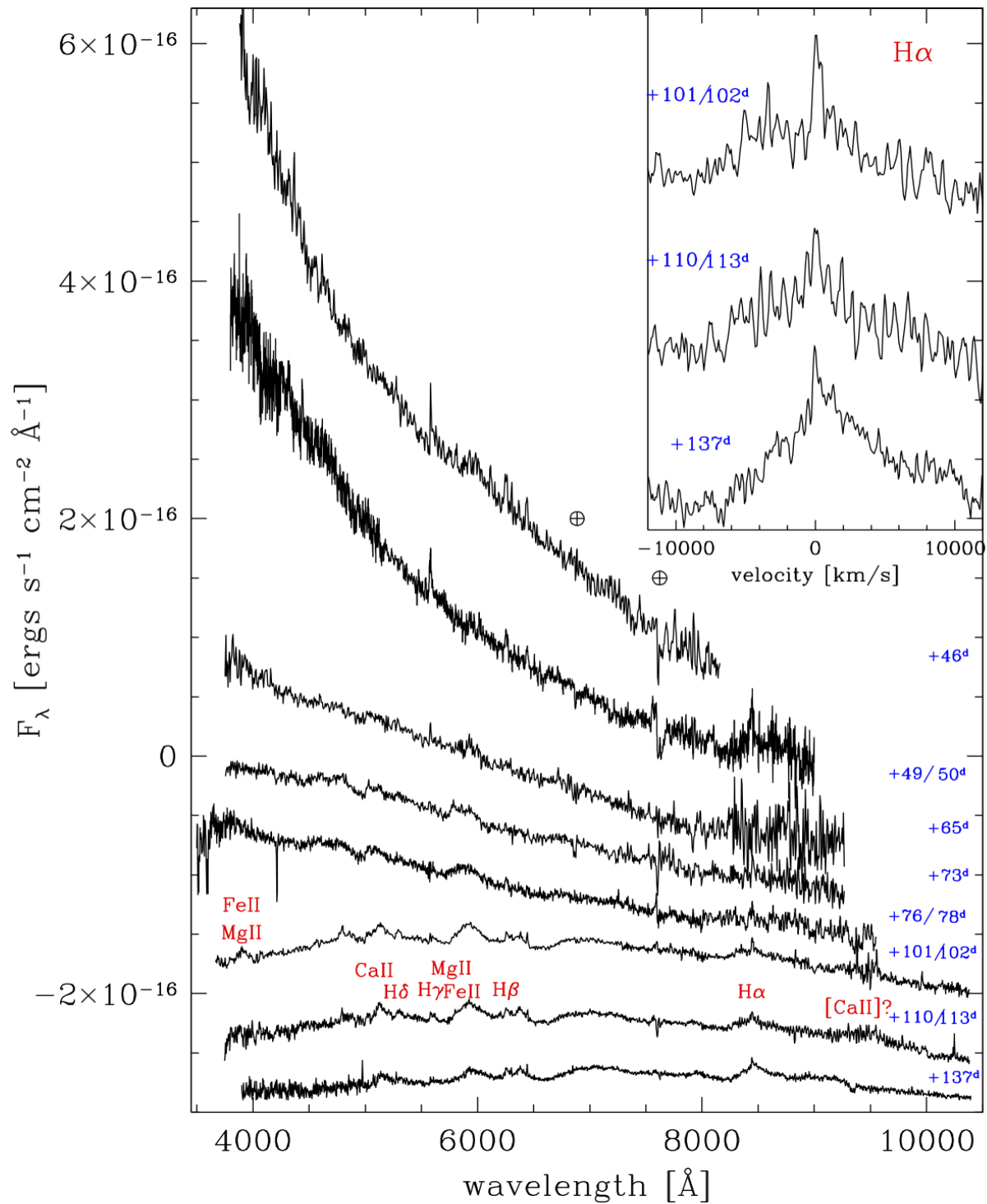


**Figure 3.** Spectral evolution of CSS121015. Wavelength and phases (from explosion) are in the observer's frame. The ordinate refers to the first spectrum, and the others have been arbitrarily shifted downwards. The +49/50 days spectrum is a merge of the AFOSC and ISIS spectra. The +65 days spectrum is the average of the AFOSC and EFOSC2 spectra. The +76/78 days spectrum is a merge of the LRS and ISIS spectra. The +101/102 days spectrum is the average of the EFOSC2 and LRS spectra. Finally, the +110/113 days spectrum is the average of two LRS spectra (see Table 4). Residuals from the atmospheric absorption corrections have been marked with the  $\oplus$  symbol. The upper-right inset shows the evolution of the H $\alpha$  profile, in velocity space.

**Table 3.** SDSS Photometry in *griz* bands, calibrated in the ABmag system.

date	JD (−2400000)	phase* (days)	<i>g</i>	err <i>g</i>	<i>r</i>	err <i>r</i>	<i>i</i>	err <i>i</i>	<i>z</i>	err <i>z</i>	instr**
20121026	56226.10	52(40)			18.42	0.12	18.25	0.18			RAT
20121030	56231.00	57(44)	18.50	0.30	18.42	0.16					Fau2
20121102	56233.90	60(47)	18.51	0.04	18.49	0.02	18.62	0.07	18.56	0.06	Fau2
20121105	56236.70	63(49)	18.62	0.04	18.52	0.02	18.58	0.07	18.59	0.04	Fau2
20121109	56240.70	67(52)	18.69	0.06	18.57	0.02	18.65	0.07	18.55	0.04	Fau2
20121111	56242.70	69(53)	18.83	0.05	18.63	0.04	18.67	0.09	18.56	0.08	Fau2
20111115	56246.80	73(57)	18.84	0.07	18.73	0.04	18.75	0.08			Fau2
20121126	56257.80	84(65)	19.18	0.09	18.78	0.13	18.76	0.10	18.83	0.10	Fau1
20121130	56261.84	88(68)			18.97	0.04	18.75	0.03			RAT
20121202	56263.70	90(70)	19.51	0.06	19.02	0.04	18.94	0.07	18.67	0.10	Fau1
20121204	56265.83	92(71)			19.10	0.03	18.91	0.03			RAT
20121205	56266.84	93(72)			19.04	0.03	18.85	0.03			RAT
20121207	56268.84	95(74)			19.21	0.04	18.91	0.06			RAT
20121209	56270.84	97(75)			19.29	0.03	18.96	0.03			RAT
20121214	56275.80	102(79)	19.96	0.08	19.31	0.08	19.03	0.09			Fau1
20121215	56276.83	103(80)			19.34	0.04	19.00	0.05			RAT
20121218	56279.86	106(82)			19.39	0.03	19.11	0.03			RAT
20121227	56288.84	115(89)			19.74	0.05	19.29	0.03			RAT
20130112	56304.82	131(102)			20.19	0.05	19.67	0.12			RAT
20130115	56307.87	134(104)			20.34	0.06	19.90	0.08			RAT
20130124	56316.86	143(111)			20.61	0.07	20.00	0.04			RAT
20130128	56320.83	147(114)			20.65	0.07	20.10	0.09			RAT
20130610	56453.75	280(217)			>22.38	0.20					ACA
20130611	56454.67	281(218)					>22.42	0.20			ACA
20130715	56488.69	315(245)			>23.1	0.30					LRS

\* - Relative to the estimated epoch of the explosion (JD = 2456174); the phase in parenthesis is in the SN rest frame.

\*\* - See note to Table 2 for instrument coding, plus:

Fau1 = Faulkes Telescope North+EM01

Fau2 = Faulkes Telescope North+fs02

ACA = WHT + ACAM

transitions of iron group elements. The spectral energy distributions (SEDs) of the SNe in our sample are very similar at all epochs<sup>7</sup>.

## 5 DISCUSSION

### 5.1 Absolute magnitudes of CSS121015 and comparison with other SLSNe

With the adopted interstellar extinction and distance discussed in Section 2, we obtain an absolute V-band magnitude at maximum of  $M_V \sim -22.9 \pm 0.1$  for CSS121015, which makes it one of the brightest SNe ever observed. Moreover, the measured V-band decline rate (see Sect. 3.1), for the given redshift, translates approximately to a rest-frame decay rate of  $\sim 4.15 \text{ mag } (100\text{d})^{-1}$  in B, typical of type II-Linear SNe (Patat et al. 1994), or a rapid decline supernova following Arcavi et al. (2012).

A comparison of the V-band light curve with those of the sample of bright SNe selected before is shown in Figure 6. The sample includes the super-bright, hydrogen-rich

transients SN 2008es (Gezari et al. 2009) and SN 2008fz (Drake et al. 2010; Agnoletto et al. 2010, Benetti et al. in preparation). We also show the type II<sub>n</sub> SN 2005gj that is spectroscopically very similar to the other SNe of the sample. We stress that SN 2005gj has been explained in terms of an interacting SN Ia (Prieto et al. 2007; Aldering et al. 2006). However this interpretation has been questioned by Benetti et al. (2006); Trundle et al. (2008); Inserra et al. (2013b) for this class of objects, since a scenario involving the interaction between an energetic SN Ic and a dense CSM could also explain the observations.

CSS121015 stands out as the brightest object in the sample. The shape of the  $M_V$  light curve is similar to that of SN 2008es, whose rise is less constrained. The SN 2008fz light curve is somewhat broader both in the rise and in the decline phase. Due to its slower evolution, the V-band luminosity of SN 2008fz matches that of CSS121015 at about 80 days after explosion. SN 2005gj is fainter by about two magnitudes than other SNe and its light curve broader.

In summary, the V-band light curve is similar to those of SNe 2008es and 2008fz, with a relatively fast luminosity decline after maximum. In canonical SNe II<sub>n</sub>, the interaction with a relatively dense CSM sustains the luminosity of the supernova until late phases, making the luminosity decline rate much slower than that expected from radioactive <sup>56</sup>Co decay (e.g., SN 1988Z, Turatto et al. 1993; Kiewe et al. 2012). In other SNe II<sub>n</sub>, e.g. SNe 1994W (Sollerman et al.

<sup>7</sup> The striking similarities of SN 2005gj to some SLSNe-II (see Fig. 5) seems to support that at least some former SNe assigned to the interacting-Ia class (but see Trundle et al. 2008; Inserra et al. 2013b, for a different interpretation), could instead be associated with the deaths of massive stars.

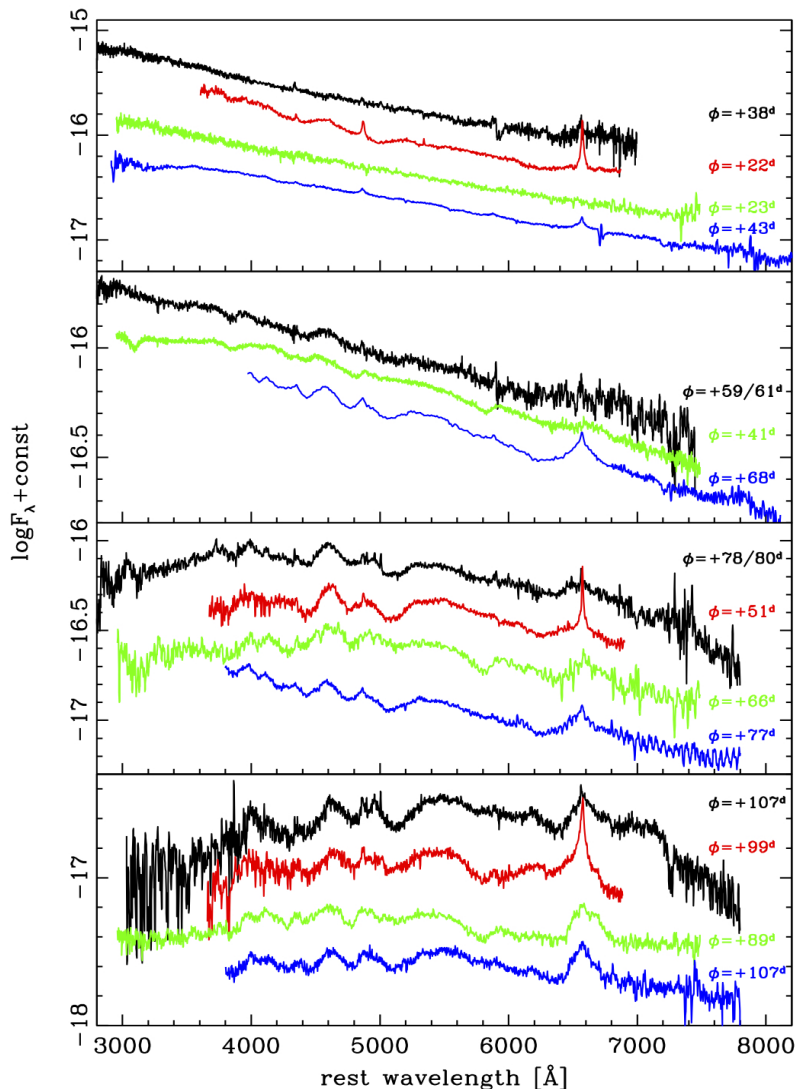


**Figure 5.** Comparison of the spectra of CSS121015 with those of a selected sample of bright SNe at significant epochs (cfr. Sect. 4.1). From top to bottom in each panel: spectra of CSS121015 (black), SN 2005gj (Prieto et al. 2007; Aldering et al. 2006, red), SN 2008es (Gezari et al. 2009; Miller et al. 2009, green) and SN 2008fz (Agoletto et al. 2010, blue). The spectra have been corrected for redshift and reddening. The rest frame phases are from the estimated dates of explosion. We plot the SN 2005gj +51 days spectrum in the +70 day panel, since this spectrum is a better match to that of CSS121015 at this epoch.

1998) and 2009kn (Kankare et al. 2012), the late-time decline is, to a first order approximation, consistent with  $^{56}\text{Co}$  decay. The fast early decline of H-rich SLSNe (SLSNe-II) is more reminiscent of SNe IIL, some of which also show signatures of early interaction, e.g. SN 1994aj (Benetti et al. 1998), SN 1996L (Benetti et al. 1999) or SN 1998S (Leonard et al. 2000; Fassia et al. 2000; Anupama et al. 2001; Fassia et al. 2001).

## 5.2 Physical interpretation of the explosion

We have presented a photometric and spectroscopic study of CSS121015, which is among the most luminous SNe ever discovered. We have highlighted photometric similarities and differences with respect to a selected sample of SLSNe-II and in general to type IIn SNe. Hereafter we elaborate on a

speculative scenario that appears to be consistent with the observations.

Let us assume that the progenitor of CSS121015 was a restless, very massive star ( $M > 50M_{\odot}$ ), that during nuclear burning ejected several solar masses of material in distinct outbursts, resulting in a number of massive circumstellar shells (see e.g. Pastorello et al. 2010a; Foley et al. 2011; Smith et al. 2011). When the star experiences a subsequent major outburst, or the final core collapse explosion, the fast expanding ejecta soon collide with the innermost massive shell, and a fraction of the kinetic energy of the ejecta is thermalized in the shell.

The shock occurs at the inner boundary of the massive, optically thick CSM shell, and in most cases will be observable only indirectly. In typical SNe IIn, the CSM is optically thin and the violent collision results in a num-

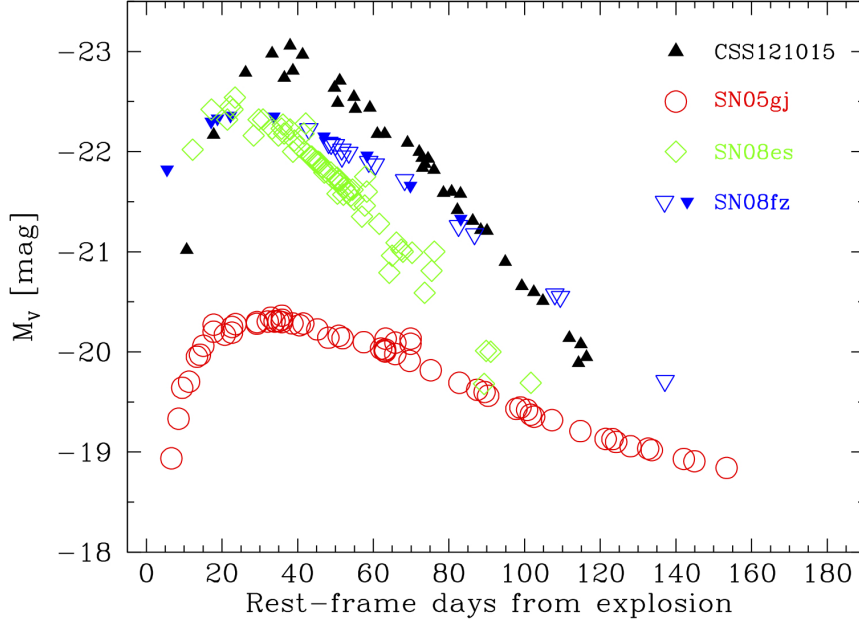


**Figure 6.** Comparison of the absolute V-band light curve of CSS121015 with those of SNe 2005gj, 2008es and 2008fz. The phases have been corrected for the time dilation due to cosmic expansion; a K-correction has not been applied. SN 2005gj is the nearest supernova ( $z = 0.06$  and photometry from Prieto et al. 2007; Aldering et al. 2006). We have adopted only Galactic absorption correction (from  $E(B-V) = 0.107$  mag, Schlafly & Finkbeiner 2011) and explosion epoch  $JD = 2453633$  (Prieto et al. 2007). SN 2008es is at a distance similar to that of CSS121015 ( $z = 0.202$  taken from the Asiago Supernova Catalogue, ASC). The photometry and explosion epoch ( $JD = 2454574$ ) are from Gezari et al. (2009) and Galactic reddening ( $E(B-V) = 0.010$  mag) from Schlafly & Finkbeiner (2011). For SN 2008fz (redshift  $z = 0.133$ , from ASC) the solid blue triangles are from Drake et al. (2010), while the empty blue triangles and explosion epoch ( $JD = 2454700$ ) are from Agnoletto et al. (2010) and Benetti et al. (in preparation). A correction for Galactic reddening of  $E(B-V) = 0.036$  mag (Schlafly & Finkbeiner 2011) has been applied.

ber of phenomena, in particularly strong X-ray and radio emission, strong optical emission lines with multiple components, including narrow features with velocity typical of the surrounding CSM, and intermediate features with FWHM of a few thousand  $\text{km s}^{-1}$ , arising from the shocked ejecta. Of course, there is room for intermediate cases such as SN 2005gj, where the CSM is dilute enough to show some of the shock phenomena, i.e. multiple-component emission lines, but not strong X-ray and radio emission (Aldering et al. 2006).

In the shock, kinetic energy is converted to radiation, and the shell is heated and accelerated. The luminosity rise time depends mainly on the radiation diffusion timescale in the shell (for CSS121015, we find a relatively long  $\sim 35$  day rest-frame rise time), while the emerging spectrum is well fitted by a blackbody at high temperature. If the shell is initially at a large distance from the star, the early adiabatic losses after collision are small, and super-luminous peak absolute magnitudes ( $M < -21$ ) are possible, provided the shell is sufficiently massive and opaque to efficiently thermalize a large fraction of the ejecta kinetic energy. This is the case for CSS121015: at maximum light, we find that the still-opaque shell has a blackbody radius of  $\sim 140$  AU (deduced from  $\log L_{\text{UBVRiz}} \sim 44.5$  dex, assuming a BB temperature of  $\sim 17700$  K). Similar opaque-shell models for SLSNe-II 2006tf and 2006gy had blackbody radii and temperatures of 300 AU and 7800 K, and 320 AU and  $\sim 10000$  K, respectively (Smith et al. 2008; Smith & Mc-

Cray 2007). Perhaps more relevant is the fit to SN 2008es from Miller et al. (2009), owing to its observed similarities with CSS121015. They found a temperature of  $\sim 15000$  K and a radius of  $\sim 260$  AU shortly after peak. The smaller radius inferred for the shell around CSS121015 implies that it was ejected either more recently in the history of the progenitor, or at lower velocity, compared to these other very luminous SNe.

At times longer than the diffusion timescale, radiation leaks out at a significant rate from the cooling shell between the forward and reverse shocks. As the shell cools, instabilities in the shocked region lead to clumping. The optical depth in the rarified inter-clump regions drops rapidly, reducing the mean opacity, and finally allowing radiation from the shocked ejecta of the SN itself to escape (Smith et al. 2008; Agnoletto et al. 2010). About eighty days after explosion, the spectra start to be dominated by broad metal features (see Fig 3), consistent with underlying Type Ic supernova shocked-ejecta. These features are relatively weak compared with that of a normal SN Ic, because in this case they appear superimposed on the extremely luminous blackbody emission from the pseudo-photosphere. These features are also very similar to those seen in SLSNe with no hydrogen in their spectra (SLSNe-Ic, cfr. Sect. 5.3).

The blackbody radius increases constantly in time, as expected for an expanding and cooling pseudo-photosphere. It reaches an extension of about 450 AU by the time of our last spectrum (see Fig. 3;  $\log L_{\text{UBVRiz}}(+107\text{d}) \sim 43.4$

**Table 4.** Spectroscopic observations of CSS121015

date	JD −2400000	phase* (days)	range (Å)	inst.**	res. (Å)
20121019	56220.38	+46(36)	3500-8200	AF	13.5
20121022	56223.29	+49(38)	3500-8200	AF	13.5
20121022	56223.62	+50(39)	3200-9000	ISI	6
20121105	56237.38	+63(49)	3500-8200	AF	13.5
20121107	56238.65	+65(50)	3650-9300	EF2	18
20121107	56239.33	+65(51)	3500-8200	AF	13.5
20121113	56244.58	+71(55)	3650-9300	EF2	18
20121115	56246.56	+73(56)	3650-9300	EF2	18
20121118	56249.50	+76(59)	3200-8000	LRS	10.5
20121120	56252.47	+78(61)	3500-9800	ISI	7
20121123	56254.59	+81(63)	3650-9300	EF2	18
20121203	56264.76	+91(71)	9500-13500	Luc	3
20121204	56266.30	+92(72)	3500-8200	AF	13.5
20121206	56267.56	+94(73)	3650-9300	EF2	18
20121209	56271.29	+97(76)	3500-8200	AF	13.5
20121213	56274.55	+101(78)	3650-9300	EF2	18
20121214	56276.46	+102(80)	3200-10000	LRS	10.5
20121222	56284.38	+110(86)	3200-10000	LRS	10.5
20121225	56287.36	+113(88)	3200-10000	LRS	10.5
20130118	56311.33	+137(107)	3600-10000	OSI	9

\* - Relative to the estimated epoch of the explosion (JD = 2456174); the phase in parenthesis is in the SN rest frame.

\*\* - See note to Table 2 for instrument coding, plus:

ISI = WHT+ISIS

Luc = LBT+Lucifer (flat continuum, noisy spectrum)

OSI = GTC+OSIRIS

dex). Taking into account that the difference between the photospheric radius at the time of our last spectrum and the radius deduced at the epoch of our first spectrum is  $\sim 4.1 \times 10^{15}$  cm, and that the time lapse between these two spectra is 68 days in the rest frame, we deduce for the pseudo-photosphere an average expansion velocity of  $\sim 7400$  km s $^{-1}$ . This is comparable to the expansion velocity derived from the broad H $\alpha$  emission. The temperature evolution of CSS121015 is reminiscent of those of normal CC-SNe, suggesting that the recombining pseudo-photosphere recedes (in mass coordinates) deeper into the dense, shocked region, while the envelope expands and cools.

In this scenario, the narrow-to-intermediate width Balmer emissions that are signatures of CSM interaction could be weak (as observed in CSS121015) or entirely absent, if the CSM shell is opaque and the shock encounters no further CSM at larger radii. As stated previously, the condition of a highly opaque shell *must* hold, in order to generate the observed continuum luminosity (Smith & McCray 2007). The fact that the spectrum remains featureless for a long time also demonstrates that there is a very high optical depth between the observer and the underlying supernova shocked ejecta. An interesting question is whether there are regimes of density/temperature/opacity where the intermediate-width Balmer lines from the shocked region are absent, i.e. can this scenario also describe SLSNe-Ic? While this seems plausible, detailed spectral modelling is necessary for a confirmation.

The FWHM of the Balmer lines are not seen to decrease significantly with time. This is probably because, due to the  $\gtrsim 30$  day diffusion time in the shell, a great deal of CSM

mass has been swept up by the forward shock before we observe any emission. Deceleration of the shocked material likely does occur at early times, following the ejecta-CSM collision. However, by the time the transient becomes visible, the massive, shocked shell coasts at constant velocity, since adiabatic losses are small at the initial radius of the interaction. The same phenomenon was observed in SN 2006tf and, according to Smith & McCray (2007), the fact that the shell does not slow down while it radiates  $\gtrsim 10^{51}$  erg shows that it must comprise at least several solar masses.

The narrow Balmer lines most likely arise from an unshocked, low-velocity wind external to the dense shell (Smith et al. 2008). The presence/density of this wind, perhaps along with the composition of the underlying ejecta (Type I vs Type II), is likely the origin of the spectral differences between CSS121015-like and 2006gy-like SLSNe-II, which display prominent, multi-component Balmer lines (Smith et al. 2007).

Since the radius deduced for CSS121015 exceeds that of typical red supergiants (Smith et al. 2001) by more than a factor of 10, we propose that the opaque CSM shell was ejected some time prior to the SN explosion and is not bound to the star. A similar model was suggested for SN 2008es for which the CSM mass was estimated between  $\sim 5 M_{\odot}$  (Miller et al. 2009) and  $\sim 2.5 - 3 M_{\odot}$  (Chatzopoulos et al. 2013).

Following the formalisms of Quimby et al. (2007) and Smith & McCray (2007) for the radiation emitted by a shocked, thermalized shell, the peak luminosity is  $L \propto \frac{1}{2} M_{\text{sh}} v_{\text{ph}}^2 / t_{\text{max}}$ , where  $M_{\text{sh}}$  is the mass of the CSM shell,  $v_{\text{ph}}$  is the velocity of the pseudo-photosphere and  $t_{\text{max}}$  is the rise time of bolometric light curve. If we assume that CSS121015 has a rise time  $\sim 1.6$  times that of SN 2008es, a peak brighter by 0.19 dex and a comparable photospheric velocity (see Fig. 5), we estimate (with the above formula) a CSM mass of  $\sim 6 M_{\odot}$ , where we have used a mass of  $\sim 2.5 M_{\odot}$  for the SN 2008es CSM shell (Chatzopoulos et al. 2013).

We can apply a consistency check on the energetics of our model. Smith & McCray (2007) note that, even with high efficiency in thermalizing the ejecta kinetic energy in the shell, momentum conservation tells us that the kinetic energy of the now-accelerated, shocked shell must be at least of the order of the thermal energy deposited. The thermal energy in the shell is eventually observed as radiation; integrating our bolometric light curve implies this is  $\gtrsim 1.7 \times 10^{51}$  erg. Taking our estimated shell mass of  $\sim 6 M_{\odot}$  and velocity of  $7400$  km s $^{-1}$ , we estimate a kinetic energy of  $\sim 3.5 \times 10^{51}$  erg, so the parameters we have derived do seem to be consistent. This also suggests that the explosion energy of the supernova was  $\gtrsim 5 - 6 \times 10^{51}$  erg.

With the derived mass, we can explain the relatively fast rise and decay observed for CSS121015, compared to other luminous, slowly-evolving SNe (e.g. SN 2006gy, Smith et al. 2007; Ofek et al. 2007; Agnoletto et al. 2009), since the radiation diffusion time for this SN will be much shorter than in those events. If we assume the mass comprising this shell was lost in a steady wind, we can estimate the mass loss rate as follows: we take the blackbody radius at maximum light ( $\sim 2 \times 10^{13}$  m) as a representative radius for the CSM shell (as the shell is optically thick, the photosphere should be near the outer edge, so this is a reasonable approximation), and a wind velocity of  $10 - 100$  km s $^{-1}$  (where the upper limit corresponds to a typical LBV wind), and find that the

wind must have began  $\sim 6 - 65$  yr before explosion. The corresponding mass loss rate is then  $\sim 0.1 - 1 M_{\odot} \text{ yr}^{-1}$ , which is much larger than any known stellar wind. Normal wind-driven mass loss therefore seems unlikely.

If instead, the mass loss occurred in an outburst like those seen in SNe 1994aj (Benetti et al. 1998) and 1996L (Benetti et al. 1999), where the CSM shell had velocities of  $\lesssim 800 \text{ km s}^{-1}$  (a similar velocity is also deduced from the barely resolved CSS121015 narrow lines), then the impulsive mass ejection would have happened only 1 year before the core collapse. This violent mass loss would have probably given rise to a pre-explosion optical transient, similar to those reported by Pastorello et al. (2007) for SN 2006jc and by Ofek et al. (2013) for SN 2010mc. The inspection of the pre-outburst light curve of CSS121015<sup>8</sup> does not show any strong activity within 7 years before the explosion. However, the deepest limiting magnitudes of the pre-CSS121015 measurements are  $\lesssim 20.6$ , which corresponds to an absolute magnitude of  $\lesssim -20.6$  mag. A massive ejection like those seen in SN 2006jc and proposed for SNe 1994aj and 1996L would have been well below the detection limit.

If we compare the luminosity upper limit at  $\sim 217 - 245$  days (rest frame) with the bolometric luminosity of SN 1987A at a similar phase, we derive an upper limit of  $\lesssim 2.5 M_{\odot}$  for the  $^{56}\text{Ni}$  mass ejected in the explosion. This value for the  $^{56}\text{Ni}$  mass is still consistent with the lower limits of  $^{56}\text{Ni}$  foreseen for some pair-instability scenario models (Whalen et al. 2013) in stars with initial masses between  $150-200 M_{\odot}$ .

In summary the observations of CSS121015 suggest that the extreme optical luminosity arises from kinetic energy thermalized in the shock between the ejecta and a dense shell. This seems to require a circumstellar shell of a few solar masses, and therefore a massive star as its progenitor. The obscuring effect of the opaque shell means that we do not get a direct view of the SN ejecta until approximately 60 days (rest frame) after explosion, making it difficult to infer the explosion mechanism. The lines that eventually appear are reminiscent of the weak SN Ic features in SLSNe-Ic. However, there is no evidence to support a pair-instability SN interpretation, and an energetic, core collapse explosion from a stripped envelope progenitor is the more natural candidate for the explosion mechanism.

### 5.3 H-poor SLSNe (SLSNe-Ic) in the context of CSS121015

We argued that the reprocessing of kinetic energy into radiation via ejecta-CSM interaction satisfactorily explains the properties of SLSNe-II. However, whether this mechanism also explains the behaviour of very luminous H-poor events is still a subject of debate. Thermonuclear explosion, triggered by pair-production in an extremely massive star, has been proposed to explain the SLSN 2007bi (Gal-Yam et al. 2009), whose late-time light curve has a slope which is consistent with  $^{56}\text{Co}$  decay. Nonetheless, a more canonical core-collapse, with the ejection of a relatively large amount of  $^{56}\text{Ni}$ , may reproduce equally well the high luminosity observed in this SN and its overall early time spectro-

photometric properties (Young et al. 2010; Moriya et al. 2010). Another group of SLSNe-Ic shows a linear decline in the late-time light curve, much faster than that expected from the  $^{56}\text{Co}$  decay (Pastorello et al. 2010b; Quimby et al. 2011; Chomiuk et al. 2011; Barbary et al. 2009; Leloudas et al. 2012; Chornock et al. 2013; Lunnan et al. 2013; Inserra et al. 2013a). This implies that these events cannot be powered by large masses of radioactive material. It has been suggested by Nicholl et al. (2013) that two recent SNe that are spectroscopically similar to SN 2007bi actually appear to be extreme members of this class, and are not consistent with extremely massive, nickel-rich ejecta, such that all SLSNe-Ic could fall into this group. If nickel decay does not drive the SLSNe-Ic, only two mechanisms can explain their properties: the energy released in the spin-down of a newly born magnetar (Kasen & Bildsten 2010; Woosley 2010), and circumstellar shock heating produced by ejecta-CSM interaction (Chatzopoulos et al. 2013, and references therein). We now investigate how our interaction view can unify the powering mechanism for all SLSNe, independent of whether they are H-rich or H-poor. Variations of this scenario have also been proposed by Blinnikov & Sorokina (2010); Chevalier & Irwin (2011); Ginzburg & Balberg (2012); Moriya et al. (2013c). Of course, it is also possible that the magnetar spin-down powers the light curves of most SLSNe, while weak interaction leads to the addition of hydrogen features in the spectra of objects like CSS121015, but we leave this discussion for a future work.

The main arguments to support the existence of a common powering mechanism for all SLSNe are observational. In Section 5.1 and 4.1, we have emphasized the striking similarity of CSS121015 with a number of SLSNe-II. Hereafter, we will show that CSS121015 shares, in addition to the extreme luminosity, an overall spectral similarity with SLSNe-Ic. It should be noted, however, that other SLSNe-II (e.g. 2006gy, 2006tf; Smith et al. 2007, 2008) do not show spectral similarity to the SLSNe-Ic. Possibly this is because they inhabit H-rich environments, where one cannot avoid H-dominated spectra with narrow lines, and/or the supernova itself is also H-rich. Interestingly, SLSNe-II seem to occur in similar dwarf galaxies to the SLSNe-Ic (Neill et al. 2011), whereas SN 2006gy was in NGC 1260 – a much more massive, redder galaxy.

In order to emphasize the similarity between CSS121015 and SLSNe-Ic, we constructed quasi-bolometric light curves for a sample of H-poor SLSNe: SN 2010gx (Pastorello et al. 2010b), SN 2011ke and SN 2012il (Inserra et al. 2013a). The pseudo-bolometric light curve of CSS121015 has been computed by integrating its multi-colour photometry from U to z, neglecting any possible contribution at low (infrared/radio) or high energy (UV, X-ray). In practice, for each epoch and filter, we derived the flux at the effective wavelength. When no observation in a given filter/epoch was available, the missing measurement was obtained through interpolation of the light curve in the given filter or, if necessary, by extrapolating the missing photometry assuming a constant colour from the closest available epoch. The fluxes, corrected for extinction, provide the spectral energy distribution at each epoch, which is integrated by the trapezoidal rule, assuming zero flux at the integration boundaries. The observed flux was converted into luminosity for the adopted distance.

<sup>8</sup> <http://voeventnet.caltech.edu/feeds/ATEL/CRTS-1210151120044133047.atel.html>

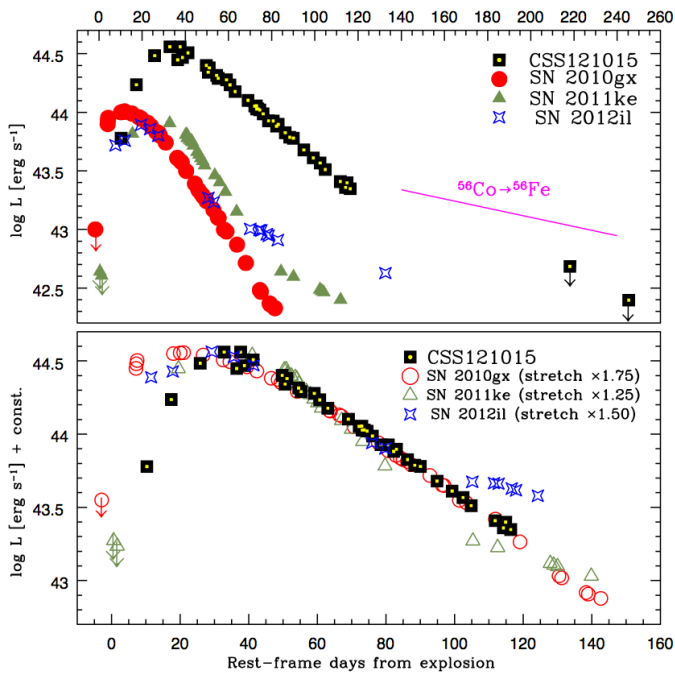


**Figure 7.** Top panel: comparison of the quasi-bolometric light curves of CSS121015 and the SLSNe-Ic 2010gx ( $z \sim 0.23$ ,  $E(B-V) = 0.04$ , from Pastorello et al. 2010b); 2011ke ( $z \sim 0.143$ ,  $E(B-V) = 0.01$ , from Inserra et al. 2013a); and 2012il ( $z \sim 0.175$ ,  $E(B-V) = 0.02$ , from Inserra et al. 2013a). The curves have been corrected for time dilatation. Bottom panel: the SLSNe-Ic light curves have been shifted in luminosity to match the peak of CSS121015, and then stretched in phase by the factors reported in the legend to approximately match its pseudo-bolometric decline.

The pseudo-bolometric light curves of this sample are presented in Fig. 7, all computed with the same prescriptions and after correction for time dilatation. The CSS121015 bolometric light curve shows a relatively fast rise to maximum of about 35 days, and slower post-maximum linear decline up to phase of about 120 days past explosion (rest frame). It reached a very bright peak of about  $\log L = 44.50$  dex. The late deep  $r$ ,  $i$  photometric limits (see Table 3) translate to an upper limit of  $\log L = 42.68$  dex. In the top panel of Fig. 7, we show the quasi-bolometric light curves for the entire sample, while in the bottom panel the light curves of SNe 2010gx, 2011ke, and 2012il have been first shifted in luminosity to match the peak of CSS121015, and then stretched in phase to match the post-peak decline of CSS121015 as closely as possible. The adopted stretch factors in the legend have been used to adjust the phases of the comparison spectra shown in Figure 8. Valenti et al. (2008), showed that stretching SNIc light curves allows an excellent description of the light curves and spectra of different objects around maximum light, in analogy we stretched the SLSNe-Ic light curves to maximize the similarity among the sample.

In Figure 8 we compare the spectra of the same objects displayed in Fig. 7. Spectra at rest frame phases of 40-50 days after the explosion are compared in the top panel, while spectra at a phase of about 3 months after explosion are compared in the bottom panel. The phases have been computed after correcting for time dilatation and applying the

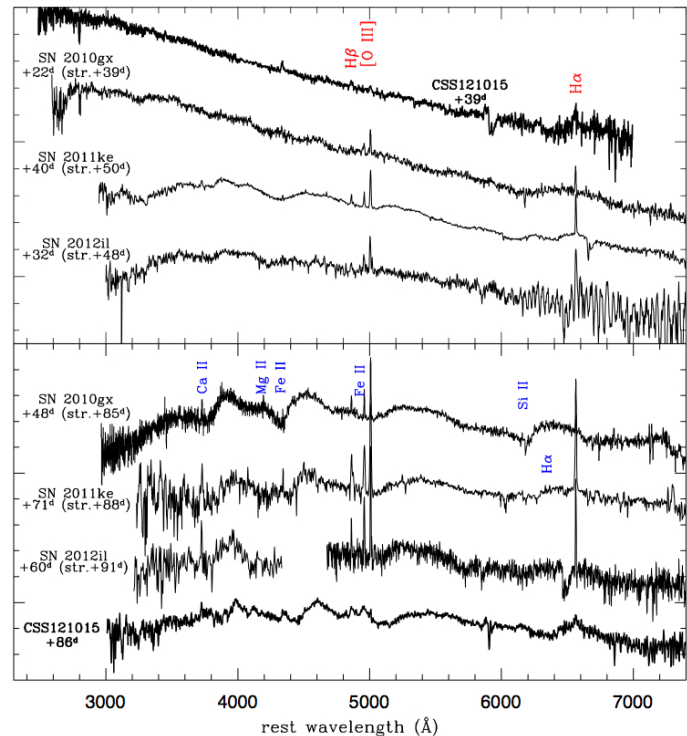


**Figure 8.** Comparison between CSS121015 and SLSNe-Ic spectra at two phases: 40-50 days after the explosion (top) and about 3 months after the explosion (bottom). The phases of SLSNe-Ic spectra have been stretched by the factors deduced from the photometry (see Section 5.3). The spectra are very similar blueward of 6000 Å. The major difference is the H $\alpha$  region, which in SLSNe-Ic is probably dominated by the Si-II 6355 Å transition. The expansion velocities seem to be similar in the entire sample.

stretch factors discussed above. In all cases, the spectra are quite similar. In particular, at 3 months, a number of common lines are detected, including Ca II, Mg II and Fe II. The overall spectral shape is also surprisingly similar in our sample spectra, with the only difference lying in the broad feature at 6300-6600 Å. This has been identified as either H $\alpha$  or Si II  $\lambda$ 6355 Å, depending on the case. In some objects (e.g. SN 2011ke), the identification of the broad feature may be disputable, with H $\alpha$  probably a more solid identification for this SN. However, while the broad H $\alpha$  has strengthened in CSS121015 from phase +38 to +86 days, the corresponding feature in SN 2011ke has weakened.

The overall spectral similarity suggests that the ejecta composition is consistent across our sample, i.e. the supernovae underlying the interactions are all of type Ic. The presence or absence of H in the spectrum is only a consequence of the shell properties – in SLSNe-Ic, the CSM is either H-deficient, or at temperature/density in which lines do not form. All known SLSNe-Ic are slow to develop type Ic features compared to normal SNe Ic (Pastorello et al. 2010b), and the presence of an initially highly-opaque shell can naturally explain why this is the case. The light curve and spectral evolution is faster for our SLSNe-Ic sample than for CSS121015, indicating shorter diffusion timescales in their shells.

All of this suggests that there may be a common power-

ing mechanism for all SLSNe. Ejecta-CSM interaction is the natural candidate for explaining the observed behaviour of SLSNe-II. However, we can clearly see that the observables of CSS121015 and other SLSNe-II have many features in common with SLSNe-Ic. For this reason, although we cannot rule out alternative explosion scenarios for the different types of SLSNe, we propose that ejecta-CSM interaction may be the most common mechanism for generating the enormous luminosities observed in SLSNe, independent of the composition (H-rich or -deficient) of their outer stellar envelopes. The diversity in the spectra between different sub-types (SLSNe-Ic and SLSNe-II, CSS121015-like and 2006gy-like) is then explained in terms of the structure and hydrogen content of their circumstellar cocoons.

## 6 CONCLUSIONS

We have presented extensive data for CSS121015, covering over 200 days (rest frame) of evolution. The collected observations, which consist of UBVR*I*griz photometry and low-resolution optical spectroscopy, make this one of the most comprehensive data sets for a SLSN.

The analysis of the observations of CSS121015 shows that this is among the brightest SNe ever discovered. Its photometric evolution is characterized by a relatively fast rise to maximum ( $\sim 35$  days in the SN rest frame), and by a post-maximum decline typical of SNe II-Linear. Its light curve shows no sign of a break to an exponential tail.

The spectral evolution is relatively fast after maximum. The first available spectrum shows a very hot ( $T_{\text{BB}} \sim 17700$  °K) and featureless continuum. The continuum cools down quickly after maximum, and the spectra show the first broad features at  $\sim 74$  days after explosion (56 days in the rest frame). A broad H $\alpha$  line is first detected at  $\sim 100$  days (80 days in the rest-frame). Narrow, barely-resolved Balmer and [O III] 5007 Å lines with decreasing flux are visible along the entire spectral evolution.

The spectra are very similar to other SLSNe-II and also to SN 2005gj, previously classified as a SN IIa (Ia interacting with H-rich CSM). The spectral similarity between SN 2005gj and SLSNe-II seems to support that at least some SNe formerly assigned to the interacting-Ia class could instead be associated with the deaths of massive stars, in agreement with Trundle et al. (2008) and Inserra et al. (2013b). CSS121015 spectra are also very similar to those of SLSNe-Ic after a phase correction, based on the relative decline rates of the (pseudo-)bolometric light curves, has been applied.

Although our analysis cannot rule out alternative powering mechanisms to explain the enormous luminosity of SLSNe (e.g. magnetar spin-down, pair instability SNe), our preferred model to explain SLSNe (with and without H) is the interaction of the ejecta with a massive, extended, opaque shell, lost by the progenitor decades before the final explosion.

**ACKNOWLEDGMENTS** S.B., E.C., A.P., L.T. and M.T. are partially supported by the PRIN-INAF 2011 with the project Transient Universe: from ESO Large to PESSTO. Research leading to these results has received

funding from the European Research Council under the European Union’s Seventh Framework Programme (FP7/2007-2013)/ERC Grant agreement n° [291222] (PI S.J.S) and EU/FP7-ERC grant n° [307260] (PI A.G.-Y.). A.G.-Y. is also supported by “The Quantum Universe I-Core program by the Israeli Committee for planning and funding and the ISF, a GIF grant, and the Kimmel award”. N.E.R. and A.M.G. acknowledge financial support by the MICINN grant AYA2011-24704/ESP, and by the ESF EUROCORES Program EuroGENESIS (MINECO grants EU12009-04170). The CRTS survey is supported by the U.S. National Science Foundation under grant AST-1313422.

This work is partially based on observations collected at: 1- the European Organisation for Astronomical Research in the Southern Hemisphere, Chile as part of PESSTO, (the Public ESO Spectroscopic Survey for Transient Objects Survey) ESO program 188.D-3003; 2- the Copernico 1.82m Telescope operated by INAF - Osservatorio Astronomico di Padova at Asiago; 3- the 3.6m Italian Telescopio Nazionale Galileo operated by the Fundación Galileo Galilei - INAF on the island of La Palma; 4- the 4.3m William Herschel Telescope operated by the Isaac Newton Group of Telescope; 5- the Gran Telescopio Canarias (GTC), installed in the Spanish Observatorio del Roque de los Muchachos of the Instituto de Astrofísica de Canarias, in the island of La Palma; 6- the Liverpool Telescope, which is operated on the island of La Palma by Liverpool John Moores University in the Spanish Observatorio del Roque de los Muchachos of the Instituto de Astrofísica de Canarias with financial support from the UK Science and Technology Facilities Council; 6- the Faulkes Telescope Project, which is an educational and research arm of the Las Cumbres Observatory Global Telescope Network (LCOGTN); 7- the Large Binocular Telescope (LBT), which is an international collaboration among institutions in the United States, Italy and Germany. The LBT Corporation partners are: The University of Arizona on behalf of the Arizona university system; Istituto Nazionale di Astrofisica, Italy; LBT Beteiligungsgesellschaft, Germany, representing the Max Planck Society, the Astrophysical Institute Potsdam, and Heidelberg University; The Ohio State University; The Research Corporation, on behalf of The University of Notre Dame, University of Minnesota and University of Virginia.

This research has made use of the NASA/IPAC Extragalactic Database (NED) which is operated by the Jet Propulsion Laboratory, California Institute of Technology, under contract with the National Aeronautics and Space Administration. We thank R. Kotak for taking the WHT+ISIS spectrum of Nov. 20th, 2012.

## REFERENCES

- Ade et al., 2013, A&A, submitted (arXiv:1303.5076)
- Agnoletto, I. et al., 2009, ApJ, 691, 1348
- Agnoletto, I., 2010, PhD Thesis, Padua University, unpublished
- Aldering, G. et al., 2006, ApJ, 650, 510
- Anupama, G. C., Sivarani, T., & Pandey, G. 2001, A&A, 367, 506
- Arcavi I., et al., 2012, ApJ, 756, L30
- Arnett, W. D. 1982, ApJ, 253, 785

- Arnett, D. 1996, *Supernovae and Nucleosynthesis* by David Arnett. Princeton University Press, 1996. ISBN: 978-0-691-01147-9
- Baltay C., et al., 2013, *PASP*, 125, 683
- Barbary, K., Dawson, K. S., Tokita, K., et al. 2009, *ApJ*, 690, 1358
- Ben-Ami S., et al., 2013, arXiv, arXiv:1309.6496
- Benetti, S., Cappellaro, E., Danziger, I. J., et al. 1998, *MNRAS*, 294, 448
- Benetti, S., Turatto, M., Cappellaro, E., Danziger, I. J., & Mazzali, P. A. 1999, *MNRAS*, 305, 811
- Benetti, S., Cappellaro, E., Turatto, M., et al. 2006, *ApJL*, 653, L129
- Blinnikov, S. I., & Sorokina, E. I. 2010, arXiv:1009.4353
- Cardelli J. A., Clayton G. C., Mathis J. S., 1989, *ApJ*, 345, 245
- Chatzopoulos, E., Wheeler, J. C., Vinko, J., Horvath, Z. L., & Nagy, A. 2013, *ApJ*, 773, 76, arXiv:1306.3447
- Chevalier, R. A., Irwin, C. M. 2011, *ApJ*, 729, L6
- Chomiuk, L., Chornock, R., Soderberg, A. M., et al. 2011, *ApJ*, 743, 114
- Chornock, R. et al. 2013, *ApJ*, 767, 162
- Cooke J., et al., 2012, *Natur*, 491, 228
- Dessart, L., Hillier, D. J., Waldman, R., Livne, E., & Blondin, S. 2012, *MNRAS*, 426, L76
- Dexter J., Kasen D., 2013, *ApJ*, 772, 30
- Drake R. P., Kuranz C. C., Miles A. R., Muthsam H. J., Plewa T., 2009, *PhPI*, 16, 041004
- Drake, A. J., Djorgovski, S. G., Prieto, J. L., et al. 2010, *ApJL*, 718, L127
- Drake, A. J., Djorgovski, S. G., Mahabal, A., et al. 2011, *ApJ*, 735, 106
- Drake, A. J., Mahabal, A.A., Djorgovski, S.G. et al. 2012, *The Astronomer's Telegram*, 4498, 1
- Drake A. J., et al., 2013, *ApJ*, 763, 32
- Eisenstein, D. J., Weinberg, D. H., Agol, E., et al. 2011, *AJ*, 142, 72
- Fassia, A., Meikle, W. P. S., Vacca, W. D., et al. 2000, *MNRAS*, 318, 1093
- Fassia, A., Meikle, W. P. S., Chugai, N., et al. 2001, *MNRAS*, 325, 907
- Foley, R. J. et al. 2011, *ApJ*, 732, 32
- Fraser, M., Inserra, C., Jerkstrand, A., et al. 2013, *MNRAS*, 433, 1312
- Gal-Yam, A. et al. 2009, *Nature*, 462, 624
- Gal-Yam, A. 2012, *Science*, 337, 927
- Gezari, S., Halpern, J. P., Grupe, D., et al. 2009, *ApJ*, 690, 1313
- Ginzburg, S., Balberg, S. 2012, *ApJn* 757, 178
- Howell D.A., D. Kasen, C. Lidman et al. 2013, *ApJ*, in press, arXiv:1310.0470
- Harutyunyan, A. H., Pfahler, P., Pastorello, A., et al. 2008, *A&A*, 488, 383
- Inserra, C., Smartt, S. J., Jerkstrand, A. et al. 2013a, *ApJ*, 770, 128
- Inserra C., et al., 2013b, *MNRAS* in press, arXiv:1307.1791
- Law N. M., et al., 2009, *PASP*, 121, 1395
- Kankare, E., Ergon, M., Bufano, F., et al. 2012, *MNRAS*, 424, 855
- Kasen, D., Bildsten, L. 2010, *ApJ*, 717, 245
- Kiewe M., et al., 2012, *ApJ*, 744, 10
- Landolt, A. U. 1992, *AJ*, 104, 340
- Leloudas, G., Chatzopoulos, E., Dilday, B., et al. 2012, *A&A*, 541, A129
- Leonard, D. C., Filippenko, A. V., Barth, A. J., & Matheson, T. 2000, *ApJ*, 536, 239
- Lunnan, R., Chornock, R., Berger, E., et al. 2013, *ApJ*, 771, 97, arXiv:1303.1531
- Margutti, R., Milisavljevic, D., Soderberg, A. M., et al. 2013, arXiv:1306.0038
- Maund, J. R. et al. 2006, *MNRAS*, 369, 390
- Mauerhan, J. C., Smith, N., Filippenko, A. V., et al. 2013, *MNRAS*, 430, 1801
- Miller, A. A., Chornock, R., Perley, D. A., et al. 2009, *ApJ*, 690, 1303
- Moriya, T. et al. 2010, *ApJ*, 717, L83
- Moriya, T. et al. 2013a, *MNRAS*, 428, 1020
- Moriya, T. et al. 2013b, *MNRAS*, 430, 1402
- Moriya, T. et al. 2013c, *MNRAS*, in press (arXiv:1307.2644)
- Neill, J. D., Sullivan, M., Gal-Yam, A., et al. 2011, *ApJ*, 727, 15
- Nicholl, M., Smartt, S. J., Jerkstrand, A. et al. 2013, *Nature*, accepted
- Ofek, E. O. et al. 2007, *ApJ*, 659, L13
- Ofek E. O., et al., 2013, *Natur*, 494, 65
- Pastorello, A., Smartt, S. J., Mattila, S., et al. 2007, *Nature*, 447, 829
- Pastorello et al. 2010a, *MNRAS* 408, 181
- Pastorello et al. 2010b, *ApJ* 724, L16
- Pastorello et al. 2013, *ApJ* 767, 1
- Patat, F., Barbon, R., Cappellaro, E., & Turatto, M. 1994, *A&A*, 282, 731
- Poznanski, D., Prochaska, J. X., & Bloom, J. S. 2012, *MNRAS*, 426, 1465
- Prieto, J. L., Garnavich, P. M., Phillips, M. M., et al. 2007, arXiv:0706.4088
- Quimby, R. M., Aldering, G., Wheeler, J. C., et al. 2007, *ApJL*, 668, L99
- Quimby, R. M., et al. 2011, *Nature*, 474, 487
- Schlafly & Finkbeiner, 2011, *ApJ*, 737, 103
- Smith, N., Humphreys, R. M., Davidson, K., Gehrz, R. D., Schuster, M. T., Krautter, J. 2001, *AJ*, 121, 1111
- Smith, N., & McCray, R. 2007, *ApJL*, 671, L17
- Smith, N., et al. 2011 *MNRAS*, 415, 773
- Smith, N., et al. 2007, *ApJ*, 666, 1116
- Smith, N., et al. 2008, *ApJ*, 686, 487
- Sollerman, J., Cumming, R. J., & Lundqvist, P. 1998, *ApJ*, 493, 933
- Tomasella, L., Benetti, S., Pastorello, A., et al. 2012, *The Astronomer's Telegram*, 4512, 1
- Tonry J. L., et al., 2012, *ApJ*, 745, 42
- Tremonti, C.A., et al. 2004, *ApJ*, 613, 898
- Trundle C., Kotak R., Vink J. S., Meikle W. P. S., 2008, *A&A*, 483, L47
- Turatto, M., Cappellaro, E., Danziger, I. J., et al. 1993, *MNRAS*, 262, 128
- Turatto M., Benetti S., Cappellaro E., 2003, *fhpc.conf*, 200
- Valenti S., et al., 2008, *MNRAS*, 383, 1485
- Van Dyk, S. D. et al., 2000, *PASP*, 112, 1532
- Whalen D. J., Joggerst C. C., Fryer C. L., Stiavelli M., Heger A., Holz D. E., 2013, *ApJ*, 768, 95
- Woosley, S. E. 2010, *ApJL*, 719, L204
- Young, D. R. et al. 2010, *A&A*, 512, 70